Astron. Astrophys. 233, 317–324 (1990)

ASTRONOMY AND ASTROPHYSICS

Do external regions of galaxies have a common orientation?

H.H. Fliche* and J.M. Souriau*

Centre de Physique Théorique**, CNRS-case 907-Luminy, F-13288 Marseille Cedex 9, France

Received September 3, 1988; accepted August 28, 1989

Abstract. We analyze the position angles of extended H I regions of galaxies. We find that contrary to the position angles estimated from the optical regions of galaxies which show a marginal now random effect, the extended H I regions are not distributed at random. Our analysis shows up a dipole anisotropy toward the direction about (5^h30mn, $+10°$). The existence of this dipole does not seem to be explained only by the flattened structure of the Supercluster. Any realistic model of galaxy formation should be able to take this phenomenon into account.

Key words: cosmology – galaxies: general – orientation of – radioastronomy

1. Introduction

It is well known that the position angles estimated from the optical regions of galaxies show a marginal non random effect, associated with the supergalactic pole (Mac Gillivray et al., 1982). However, warps are often seen and this phenomenon allows the external region of galaxies to have a different orientation of that of the central region. Hence, the statistical investigation of the position angles estimated from the 21 cm maps would yield to new results

In the present paper we discuss a sample of 83 galaxies for which the position angle of the outermost parts are obtained from 21-cm line observations. Using a Kolmogorov-Smirnov test we will show that there is a tendency to parallelism of their orientation and will refine the position of the corresponding pole using variations of statistical tests. The relation of this pole with the supergalactic pole and a "cosmic" pole found on the distribution of quasars will be noticed in the conclusion.

2. The data

The sample used in this paper includes 83 galaxies with radio data taken from the literature. The relevant data relative to this sample are given in Table 1. In column 1 is a galaxy name (NGC, IC, UGC, DDO or Anonymous number). The right ascension and declination are in columns 2 and 3. The position angles (α), which are the oriented angles between the northern direction and the major axis of the radio map are given in column 4. These angles are measured from the North to the East. We have adopted the position angles given in the original papers each time that they were published. If no α was available we performed our own measurement on radio maps. The accuracy of these measurements depends on the shape of the external contour of the maps. If the external shape is very irregular, errors in α can be rather large. References to the original papers and radio observatories are in columns 5 and 6.

3. Statistical analysis of the sample

In this section we test the null hypothesis of isotropic orientation of the H I envelopes of galaxies. We first use a Kolmogorov-Smirnov test and find that the null hypothesis can be rejected at a very high propability level (Sect. 3.1). We shall see that the best description is given by an anisotropic dipole. In Sect. 3.2, we use Gaussian statistics to extract the information content on position angles.

3.1. Non-parametric statistics

If the null hypothesis is correct, i.e. if the orientation angles of the galaxies in space are randomly distributed, the position angles are also random, and there is equipartition of the position angle α in the range 0°–180°.

This can be shown on a cumulative diagram of position angles. In Fig. 2 we have simulated such a histogram using 83 random values taken in the interval 0°–180°.

Figure 3 is a similar diagram but with the real position angles of the H I galaxy clouds taken in Table 1. The histogram in Fig. 3 differs from Fig. 2 in two aspects: first it is curved and secondly, objects near $\alpha = 90°$ are missing.

This difference can also be seen on a histogram $|\alpha - 90°|$ (Fig. 4) which shows that this variable is largely below the diagonal – the maximum vertical difference is $\Delta = 0.298$.

Is this difference significant? The Kolmogorov-Smirnov test tells us that in the null hypothesis of isotropy, the probability that a deviation $\geqq \Delta$ is found in a sample of n objects is given by:

$$p_n(\Delta) \sim 2 \sum_{j=0}^{\infty} (-1)^j \exp\left(-2\left[\left(\sqrt{n} + 0.12 + \frac{0.11}{\sqrt{n}}\right)(j+1)\,\Delta\right]^2\right).$$

Send offprint requests to: H.H. Fliche

* Université de Provence

** Laboratoire Propre, LP 7061

Table 1. The sample

Nom	Asc.	Decl.	α	Ref.	Observatories, remarks
IC10	0 17.6	+5902	43	1	Jodrell Bank
NGC224	0 40.0	+4100	33	2	Cambridge, M31
NGC247	0 44.5	-2100	176	37	Effelsberg
NGC253	0 45.1	-2534	51	3	Owens Valley
NGC300	0 52.5	-3757	162	4	Owens Valley
NGC598	1 31.1	+3024	21	5	Owens Valley, M33
NGC628	1 34.0	+1532	25	40	Westerbork, M74
NGC660	1 40.4	+1323	160	7	NRAO
IC1727	1 44.6	+2705	150	7	NRAO
NGC672	1 45.0	+2711	65	7	NRAO
NGC772	1 56.5	+1846	130	7	NRAO
NGC784	1 58.4	+2835	0	7	NRAO
NGC891	2 19.4	+4207	23	8	Westerbork
NGC925	2 24.3	+3321	115	7	NRAO
IC239	2 33.3	+3845	147	9	Cambridge
NGC1058	2 40.4	+3708	165	43	Westerbork
IC342	3 42.0	+6757	39	10	Cambridge
UGC2885	3 49.8	+3828	44	39	Westerbork
A0355	3 55.0	+6700	125	7	NRAO
NGC1530	4 17.0	+7512	0	7	NRAO
NGC1560	4 27.1	+7147	25	7	NRAO
NGC1961	5 36.6	+6921	90	11	Westerbork
NGC2146	6 10.5	+7822	160	12	NRAO
NGC2336	7 18.5	+8016	0	7	NRAO
NGC2366	7 23.6	+6918	35	7	NRAO, DDO42
NGC2403	7 32.0	+6543	125	13	Owens Valley
NGC2541	8 11.0	+4913	170	7	NRAO
A0813+70	8 14.1	+7052	175	14	Cambridge, DDO50
NGC2655	8 49.0	+7825	145	15	Effelsberg
NGC2683	8 49.6	+3336	35	7	NRAO
NGC2712	8 56.2	+4506	162	16,38	Effelsberg
NGC2715	9 01.9	+7817	163	15	Effelsberg
NGC2805	9 16.3	+6419	130	17	Westerbork; α HI: 270°
NGC2841	9 18.5	+5112	160	18	Westerbork
NGC2903	9 29.5	+2142	26	37	Effelsberg
NGC3031	9 51.4	+6918	152	19	Westerbork, M81
NGC3109	10 00.8	-2555	93	20	Effelsberg, DDO236
NGC3198	10 16.9	+4549	32	18	Westerbork
IC2574	10 24.8	+6840	45	7	NRAO, DDO81
NGC3338	10 39.5	+1400	90	7	NRAO
NGC3359	10 43.3	+6330	172	21	NRAO
NGC3368	10 44.1	+1205	170	7	NRAO, M96
NGC3521	11 03.2	+0015	155	7	NRAO
NGC3718	11 29.9	+5326	13	36	Westerbork
NGC3729	11 31.9	+5324	9	36	Westerbork
NGC3938	11 50.2	+4423	20	22	Westerbork
NGC3953	11 51.1	+5236	10	7	NRAO
NGC3998	11 55.3	+5544	15	41	Westerbork
NGC4038/9	11 59.3	-1836	5	23	Westerbork, "Antennae"
NGC4096	12 03.4	+4745	0	7	NRAO
NGC4151	12 08.0	+3941	19	24	Westerbork
NGC4214	12 13.0	+3635	150	37	Effelsberg
NGC4236	12 14.4	+6945	163	13	Owens Valley
NGC4244	12 15.0	+3805	45	37	Effelsberg
NGC4258	12 16.5	+4735	152	25	Westerbork, M106
NGC4262	12 17.0	+1519	29	42	Westerbork, ring HI
NGC4395	12 23.4	+3349	154	37	NRAO
NGC4449	12 25.8	+4422	45	26	Westerbork
NGC4490/85	12 28.1	+4155	155	20	Effelsberg
NGC4535	12 31.8	+0828	0	6	Arecibo
NGC4559	12 33.4	+2814	157	37	Effelsberg
NGC4618/25	12 39.1	+4126	35	20	Effelsberg
NGC4631	12 39.7	+3249	86	27	Westerbork
NGC4725	12 48.0	+2546	35	35	Westerbork,Jodrell Bank
NGC4736	12 48.5	+4123	114	29	Westerbork, M94
NGC4747	12 49.3	+2602	46	35	Westerbork (α:30 or 46)
DDO154	12 51.6	+2725	39	37	Effelsberg
NGC4826	12 54.2	+2157	115	7	NRAO, M64
NGC5033	13 11.2	+3651	160	18	Westerbork
NGC5055	13 13.5	+4217	116	18	Westerbork, M63
NGC5194	13 27.8	+4727	170	30	Westerbork, M51
NGC5236	13 34.2	-2937	172	31	Effelsberg, M83
NGC5301	13 44.4	+4622	174	38	Westerbork, Effelsberg
NGC5364	13 53.7	+0516	30	6	Arecibo
NGC5383	13 55.0	+4205	85	32	Westerbork, MARK281
NGC5457	14 01.5	+5435	35	33	Effelsberg, M101
NGC5832	14 58.0	+7150	71	38	Effelsberg
NGC6384	17 30.0	+0706	30	6	Arecibo
NGC6503	17 49.9	+7010	125	7	NRAO
NGC6946	20 33.8	+5959	62	34	Owens Valley
NGC7331	22 34.8	+3410	167	18	Westerbork
NGC7640	23 19.7	+4035	165	7	NRAO
A2359-15	23 59.4	-1545	0	7	NRAO, DDO221

1 Cohen, R.J.: 1979, Monthly Notices Roy.Astron.Soc. 187,839
2 Newton, K.,Emerson,D.T.:1977, Monthly Notices Roy.Astron.Soc. 181, 573
3 Combes, F., Gottesman, S.T., Weliachew, L.: 1977, Astron.Astrophys. 59, 181
4 Rogstad, D.H., Crutcher, R.M.,Chu, K.: 1979, Astrophys. j. 229, 509
5 Rogstad, D.H.,Wright, M.C.H., Lockhart, I.A..: 1976, Astrophys. j. 204, 703
6 Briggs, F.H.,Wolfe, A.M., Krumm, N., Salpeter,E.E.: 1980,Astrophys. j.238, 510
7 Rots, A.H.: 1980,Astron.Astrophys. Suppl. Ser. 41, 189
8 Sancisi, R., Allen, R.J.: 1979,Astron.Astrophys. 74, 73
9 Allsop, N.J.: 1979, Monthly Notices Roy.Astron.Soc. 187, 537
10 Newton, K.: 1980, Monthly Notices Roy.Astron.Soc. 191, 615
11 Shostak, G.S.,Hummel, E., Shaver, P.A., Van Der Hulst, J.M.,Van Der Kruit, P.C.: 1982,Astron.Astrophys. 115, 293
12 Fisher, J.R., Tully, R.B.: 1976,Astron.Astrophys. 53, 397
13 Shostak, G.S.: 1973, Astron.Astrophys. 24, 411
14 Cottrell, G.A.: 1976, Monthly Notices Roy.Astron.Soc. 177, 463
15 Huchtmeier, W.K., Richter, O.G.: Astron.Astrophys. 1982, 109,331
16 Krumm, N., Shane, W.W.: 1982, Astron.Astrophys.116, 237
17 Bosma, A., Casini,C.,Heidmann,J.,Van Der Hulst, J.M.,Van Woerden,H.: 1980, Astron.Astrophys. 89,345
18 Bosma, A.: 1981, Astron.j. 86, 1791
19 Rots,A.H.,Shane,W.W.: 1975, Astron.Astrophys. 45,25
20 Huchtmeier, W.K.,Seiradakis,J.H.,Materne,J.: 1980, Astron.Astrophys. 91,341
21 Gottesman,S.T.: 1982, Astron.j. 87,751
22 Van Der Kruit,P.C.,Shostak,G.S.: 1982, Astron.Astrophys. 105, 351
23 Van Der Hulst, J.M.: 1978 ,in I.A.U. Symposium n°77 "Structure and properties of nearby galaxies", Ed.Berkhuisjen,E.M.,Wielebinski,R. p.269
24 Bosma,A.,Ekers,R.D.,Lequeux, J.: 1977 , Astron.Astrophys. 57 ,97
25 Van Albada, G.D.,Shane,W.W.: 1975 , Astron.Astrophys. 42 , 433
26 Van Woerden,H.,Bosma,A.,Mebold,U.: 1975 , Coll.internat.C.N.R.S. N°241, Ed. Weliachev,L.,p.483
27 Weliachev,L.,Sancisi,R.,Guelin,M.: 1978, Astron.Astrophys. 65,37
28 Haynes,M.P.: 1979, Astron.j. 84, 1830
29 Bosma,A., Van Der Hulst, J.M.,Sullivan,W.T.: 1977,Astron.Astrophys.57 ,373
30 Shane,W.W.: 1975,Coll.internat.C.N.R.S. N°241, Ed. Weliachev,L.,p.217
31 Huchtmeier, W.K.,Bohnenstengel,H.D.: 1981, Astron.Astrophys. 100,72
32 Sancisi, R., Allen, R.J.Sullivan,W.T.: 1979, Astron.Astrophys. 78, 217
33 Huchtmeier, W.K.,Witzel,A.: 1979, Astron.Astrophys. 74, 138
34 Rogstad,D.H.,Shostak,G.S.: 1973, Astron.Astrophys.22, 111
35 Wevers,B.M.H.R., Appleton,P.M., Davies, R.D., Hart, L.: 1984, Astron.Astrophys. 140, 125
36 Schwarz,U.J.: 1985, Astron.Astrophys. 142, 273
37 Huchtmeier, W.K.,Seiradakis,J.H.: 1985, Astron.Astrophys. 143, 216
38 Huchtmeier, W.K., Richter, O.G.: 1984, Astron.Astrophys. 149, 118
39 Roeffsema,P.R., Allen,R.J.: 1985, Astron.Astrophys.146, 213
40 Shostak,G.S.,Van Der Kruit,P.C.:1984, Astron.Astrophys. 132, 20
41 Knapp,G.R.,Van Driel,W., Van Woerden,H.: 1985, Astron.Astrophys.142, 1
42 Krumm,N., Van Driel,W., Van Woerden,H.: 1985,Astron.Astrophys. 145, 202
43 Van Der Kruit,P.C., Shostak,G.S.: 1984, Astron.Astrophys.134, 252

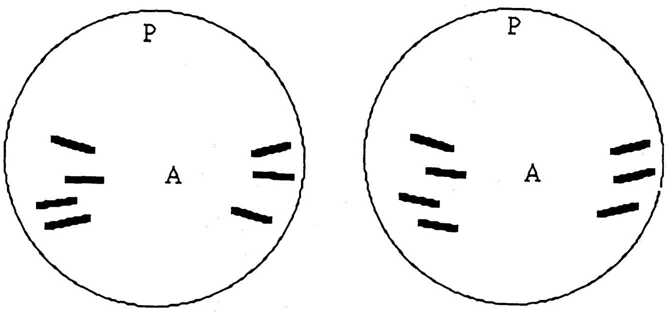

Fig. 1. In case of a non uniform distribution of the galaxies in the sky, the objects might show simultaneously a radial alignment toward a pole A and concentric toward a pole P

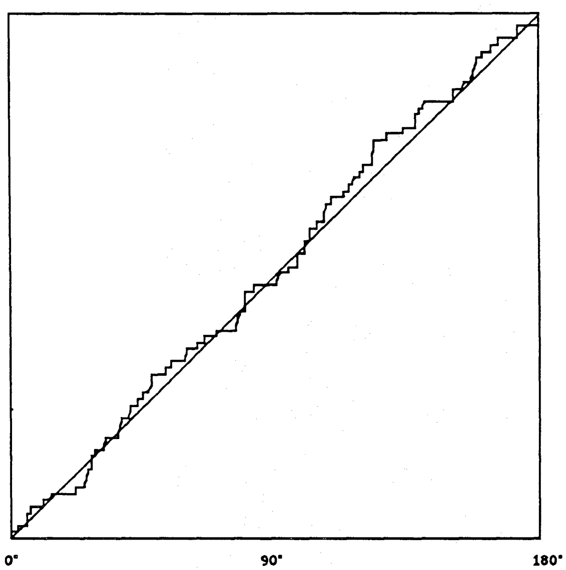

Fig. 2. Cumulative distribution function of position-angles: simulation of 83 p.a. uniformly distributed

In the present case, $n = 83$, we find the probability:

$$p_{83}(0.298) = 5\ 10^{-7}$$

thus the null hypothesis can be rejected with a 2000000 vs. 1.

The test indicates that the preferential values of the position angles are near 0° or 180° or in others words near the meridian toward the north. What can be the interpretation of such a distribution in α?

It might be possible that galaxies are aligned toward a point A, rather close to the terrestrial northern pole. We have tested this hypothesis by using random positions of A and consequently of angles α_A relative to the A direction. A set of 10000 point was randomly distributed on the sky and the value of the maximum deviation Δ was calculated for each of them. We find that the maximum of Δ is reached for

$$\text{A: (RA} = 305°,\ \text{Dec} = +80°)\ .$$

In that direction we have $\Delta = 0.316$, and the associated probability is:

$$p_{83}(0.316) < 10^{-7}\ .$$

Our results are shown in Fig. 5, where we use stereographic coordinates. On this wide angle representation of the sky, the points exterior to the dashed circle are "behind the observer". The curves are for constant values of Δ and $p(\Delta) < 0.5$. The differences between successive curves are constant.

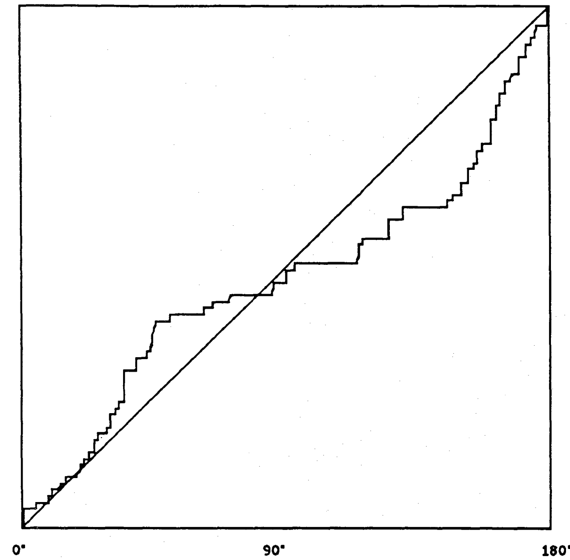

Fig. 3. Cumulative distribution function of observed position-angles

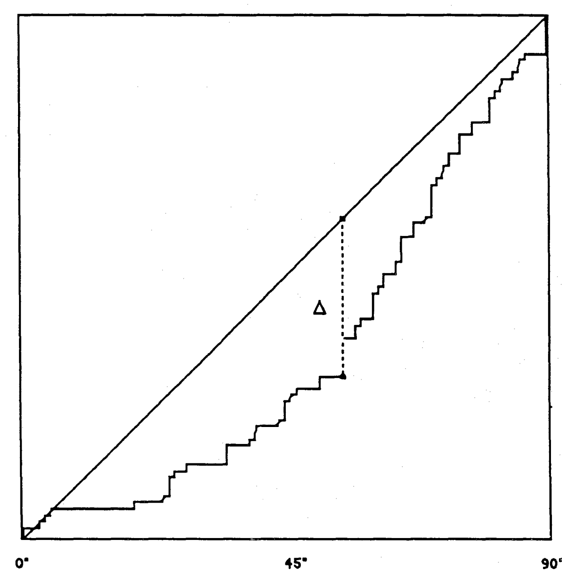

Fig. 4. Cumulative distribution function of $|\alpha - 90°|$. The value of Δ intervenes in the Kolmogorov-Smirnov's test

We notice that the relevant region can be divided in two parts:
1) a central area having 90° × 70° in size;
2) a concentric corona (the northern and southern poles are on this corona), which is itself separated in two antipodal "crescents".

This two areas correspond to a change in the sign of Δ; in the central area the α_P histograms are located above the diagonal. The case $P_1 = (91°, +9°)$ is shown in Fig. 6. In this case the maximum in Δ is in the central region. The galaxy position angles relative to P_1 are near 90°: in other words the major axis of these galaxies are on parallel relative to this pole.

It appears that the statistical orientation of galaxies can be either an alignment toward a "node" A or concentric around a

Fig. 5a. Contour map of the significance level as given by the Kolmogorov-Smirnov's test. We use stereographic coordinates. On this wide angle representation of the sky, the points exterior to the dashed circle are "behind the observer". The curves are for constant values of Δ and $p(\Delta)<0.5$. The differences between successive curves are constant

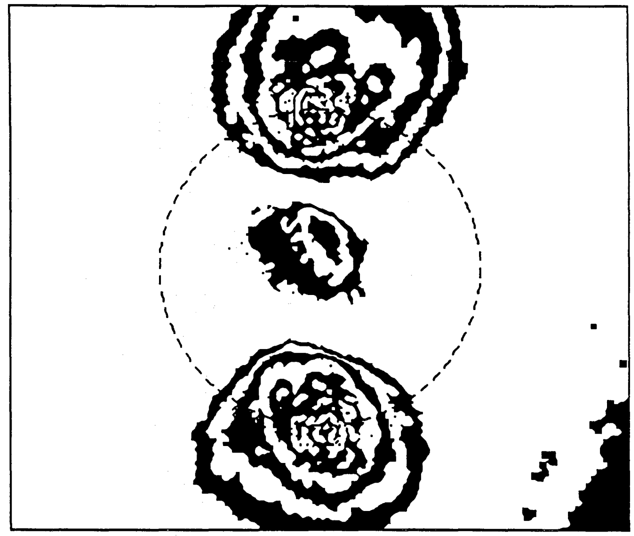

Fig. 5c. Identical to Fig. 5b but an alignment on great circles with a node A

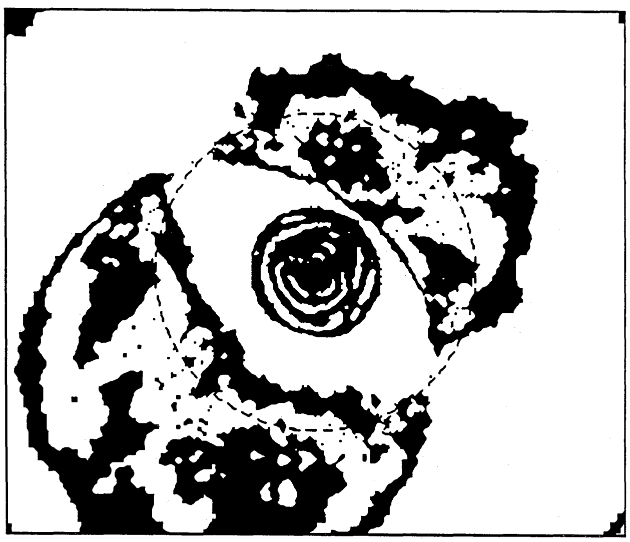

Fig. 5b. Comparison for Fig. 5a: a simulation of an alignment of the same objects on parallels with a pole P

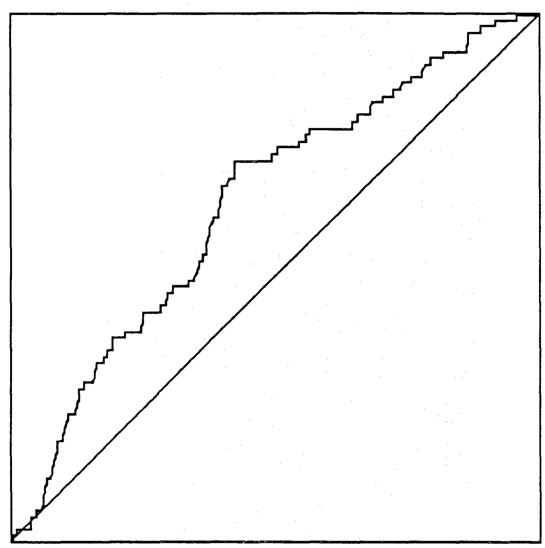

Fig. 6. Cumulative distribution function of $|\alpha-90°|$ where α is the p.a. with respect to the pole P_1

"pole" P. This can be understood with the help of Fig. 1 as follows: most of the galaxies in our sample are on an equatorial belt of pole P. This is very likely a selection effect due to the shape of the Local Super Cluster (see Sect. 3.3). The point A is on this disk far away from the galaxies. Thus the radial alignment toward A and the concentric alignment around P are close one to each other.

The best interpretation can be obtained by using two simulated samples. In the first one all position angles α_A are equal to 0° toward A, while in the other $\alpha_P = 90°$ for a point P_0 in the central region of Fig. 5a. The coordinates of the objects are the same in the real and in the two simulated samples. We use the same procedure for the simulated samples as we did for the real data. This gives Fig. 5b, in the case $\alpha_P = 90°$ and Fig. 5c for $\alpha_A = 0°$. We see immediately that Fig. 5b only appears similar to Fig. 5a. Therefore the statistics of observed position angles is best described by a concentric alignment on parallels with a pole P_0 located in the central region of Fig. 5a, with some statistical dispersion.

This result will be discussed and improved in the next section by using Gaussian statistics.

3.2. *Tests using Gaussian statistics*

The main advantage of a non parametric statistical test such as the Kolmogorov-Smirnov test is to give robust conclusions to the first order: the hypothesis of isotropy is not compatible with the observations. More accurate results can be obtained by filtering out the noise in our data. More specifically the very irregular appearance of Fig. 5a (and even Fig. 5b) is very probably due to noise superimposed on a useful signal, this noise coming from the very irregular spatial distribution of the sample.

3.2.1. First filtering

In order to filter out this noise we will use a smooth function and replace $|\alpha_P - 90°|$ by $|\cos\alpha_P|$. Statistics done on the variable $|\alpha_P - 90°|$ can be repeated on $|\cos\alpha_P|$ as well. We choose the cosine function because it has no singularity in the 0° 180° interval. Then for each position P we calculate the mean value of $|\cos\alpha_P|$ instead of $|\alpha_P - 90°|$. The isocurves now obtained (Fig. 7) are much smoother than in Fig. 5a. Moreover the central region is much smaller and very well defined. At the central point P_2: (81°, 13°) the mean value is $\langle \Delta(P_2) \rangle = 0.467$.

Is this result significant? If the hypothesis of isotropy (i.e. of equipartition of α_P) were true, the mean value of $|\cos\alpha_P|$ would be

$$\frac{1}{\pi}\int_0^\pi |\cos\alpha|\,d\alpha = \frac{2}{\pi} = 0.6366$$

and the dispersion

$$\sigma = \sqrt{\frac{1}{\pi}\int_0^\pi \cos^2\alpha\,d\alpha - \frac{4}{\pi^2}} = 0.30776\,.$$

Because $n = 83$ is sufficiently large the distribution in Δ is almost Gaussian, with the dispersion $\sigma_{83} = \sigma/83$. If we compare $\langle \Delta(P_2) \rangle = 0.467$ obtained for P_2 with the expected mean value $2/\pi$ under the null hypothesis of isotropy or equipartiition of α_P, we find that $\langle \Delta(P_2) \rangle$ is at

$$\langle \Delta(P_2) \rangle - \frac{2}{\pi} = 5.00\,\sigma_{83}$$

below the mean value. This corresponds to a probability:

$$1 - \text{erfc}\,(5.00) = 3\;10^{-7}$$

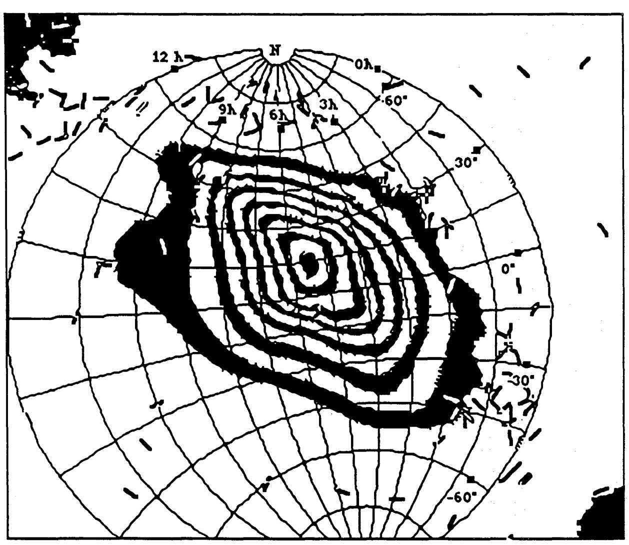

Fig. 7. Contour map of the average of $|\cos\alpha_P|$ as function of the pole P. The sky is describe in "wide-angle" stereographic coordinates: the central contour is also seen at the antipole "behind" the observer. Each galaxy with its orientation is represented twice (normal and antipodal position) since theses two points have the same rule in finding a pole direction

or in other words the hypothesis of isotropy is rejected at 3000000 against 1. This result is consistent with the Kolmogorov-Smirnov test.

To illustrate our result the Fig. 7 has been directly scaled in probabilities: the outermost curve corresponds to a probability of 1/2 and this value decreases by a factor of 10 for each concentric black region.

This gaussian test reinforces the conclusions obtained in Sect. 2.

3.2.2. Second filtering

Some irregular features are still present in Fig. 7. They are mostly due to galaxies near the pole or its antipode. When a galaxy G is near the pole a small change in P gives a large variation in position angle α_P and then a perturbation in Δ.

This effect can be removed by weighting the mean with a smooth function of the angular separation GP chosen such as $p = 0$ when $GP = 0$. We shall use:

$$p = \sin^2(GP)$$

which is undoubtedly very smooth.

The only change in statistics is in the value of the dispersion σ which is now:

$$\sigma\,\frac{\sqrt{\sum_{j=1}^{n} p_j^2}}{\sum_{j=1}^{n} p_j}\,.$$

The variation of the correction factor over the sphere is small (its value at the center of figure is 1.018).

The curves of equiprobability obtained by using this weighting function are now very regular as shown in Fig. 8a and in the enlargement of the central region (Fig. 8b); this last algorithm removes well the noise due to the spatial distribution of the sample. The lowest probability

$$1 - \text{erfc}\,(5.06) \approx 2\;10^{-7}\,,$$

is reached for the pole P_0: (81°, +8°).

We can test this result by using two simulated samples having the same coordinates: the first with random position angles, and second with $\alpha_{P_0} = 90°$ for all position angles. We apply the algorithm to the two simulated samples as to the real sample and get the following results which are displayed in Figs. 9 and 10 respectively. The shapes of equiprobability curves in Fig. 9 do not resemble those of the real data. The interpretation is obvious: since there is no information on the distribution in position angles, filtering out the simulated data leaves some noisy features, located in regions of highest spatial density. Contrary to Fig. 9 the second simulated sample is similar to that obtained in Fig. 8b for the real data (significant ellipticity in the direction NW–SE; we use conformal coordinates). To adjust equiprobability curves in Fig. 10 a correction factor of 3.4 was applied to the dispersion.

An important point coming from this simulation is that if the true distribution angle were more complicated than the one we describe (for example a multipole or evolutive), the central region in Fig. 8b would not be the same as in Fig. 10 which strictly corresponds to the simulation of a dipole.

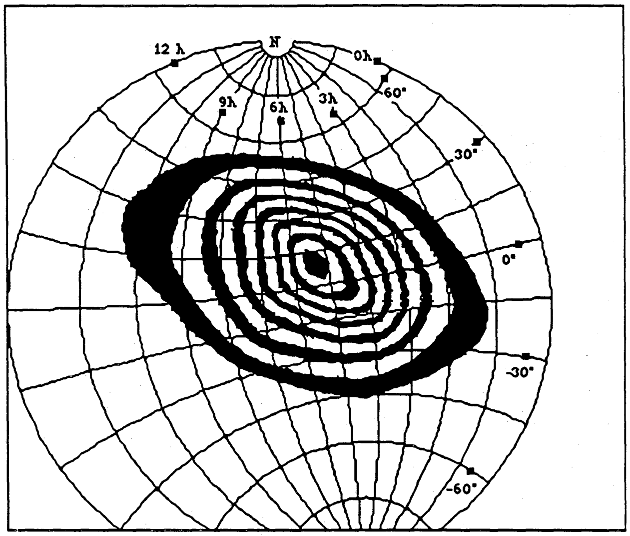

Fig. 8a. As in Fig. 7 but the are weighted for noise filtering (see text)

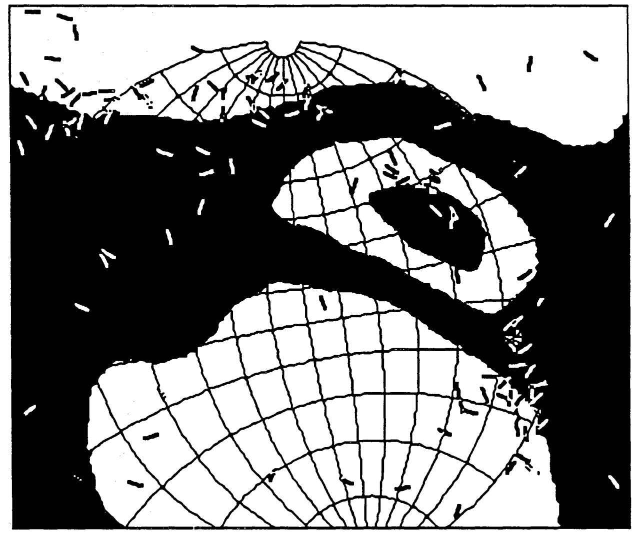

Fig. 9. Standard of Fig. 8; the contour levels correspond to random p.a., the position of the galaxies is drawn

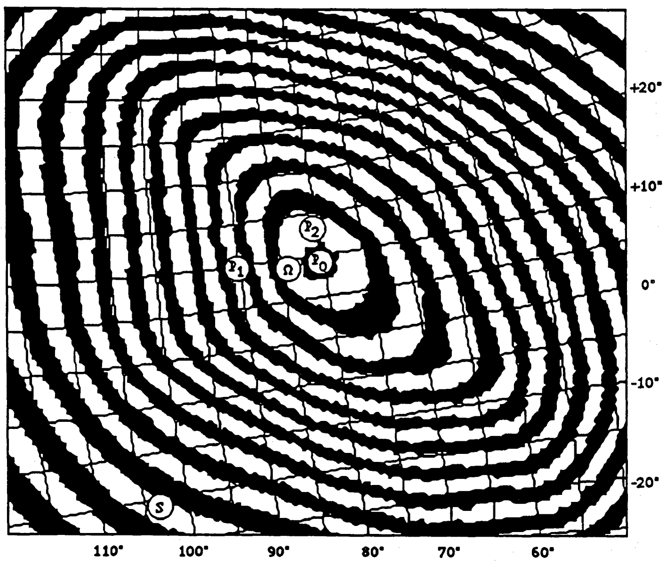

Fig. 8b. Enlargement of the central region of Fig. 8a, the indicated poles are: P_0 given by the maximum of the weighted averages; S: the supergalactic pole; Ω: the "cosmic" pole; see the text

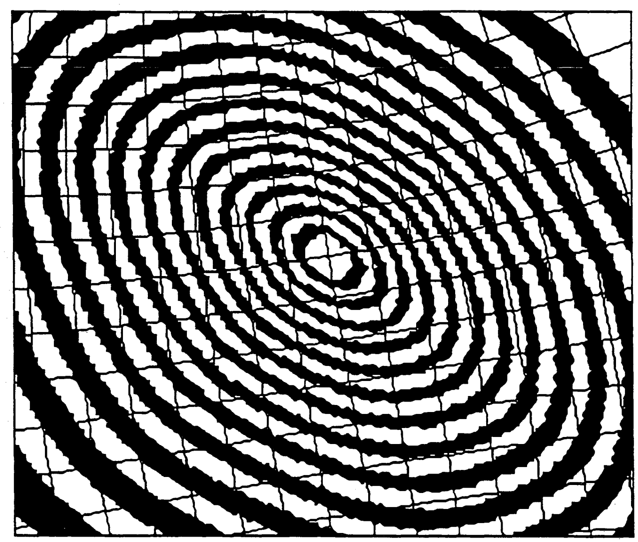

Fig. 10. Concentric simulation with respect to the pole P_0; to be compared with Fig. 8b which is obtained with the real p.a.

3.2.3. Stability in the pole determination

The statistical information content on the position angles in our sample is that of a concentric alignment around a pole P_0. The dispersion can be studied by means of Table 2.

Galaxies in this table are ranked by increasing values of $|\alpha_P - 90°|$. The anisotropy is immediately checked by using steps of 15° and counting the number of objects per steps (27, 18, 16, 7, 7, 8). We also verify that no obvious subsample is responsible of the observed anisotropy (it would populate the beginning of the table). It neither depends on observatories nor on distance of the objects. In particular there are respectively 10 and 15 galaxies in each half of the among those located in the Local Cloud as defined by de Vaucouleurs. As a consequence the anisotropy is not a local effect.

A previous determination of the dipole anisotropy (Fliche et al., 1983b), based upon a smaller sample and less elaborated statistics gave a pole at (90°, 0°). In the present paper a variety of statistical tests give the following values:

$$P_1: (91°, +9°), \quad P_2: (81°, +13°), \quad P_0^{83}: (81°, +8°),$$

the last value being probably less affected by noise. These poles which are marked in Fig. 8b, give an idea of the fluctuations due to the choice of the statistical test.

3.3. Summary

The information content of this sample can be summarized as follows:

Table 2. List of galaxies ranked for increasing |ap − 90°|, in the case of a pole P: (81°, +8°)

	αp-90°	Asc	Decl	α	Observatories, remarks
1	0	09 18.5	+51 12	160	Westerbork
2	0	11 59.3	-18 36	5	Westerbork,"Antennae"
3	1	22 34.8	+34 10	167	Westerbork
4	-1	11 51.1	+52 36	10	NRAO
5	2	08 49.0	+78 25	-35	Effelsberg
6	2	13 34.2	-29 37	-8	Effelsberg, local cloud
7	-2	07 32.0	+65 43	125	Owens Valley, local cloud
8	2	11 31.9	+53 24	9	Westerbork
9	3	00 52.5	-37 57	-18	Owens Valley, local cloud
10	-3	10 43.3	+63 30	-8	NRAO
11	-3	14 01.5	+54 35	35	Effelsberg, local cloud
12	-4	02 19.4	+42 07	23	Westerbork
13	4	11 55.3	+55 44	15	Westerbork
14	4	08 56.2	+45 06	-18	Effelsberg
15	-4	05 36.6	+69 21	90	Westerbork
16	-5	03 49.8	+38 28	44	Westerbork
17	5	12 08.0	+39 41	19	Westerbork
18	7	11 29.9	+53 26	13	Westerbork
19	-8	23 19.7	+40 35	165	NRAO
20	-9	09 51.4	+69 18	-28	Westerbork,local cloud
21	9	11 50.2	+44 23	20	Westerbork
22	10	23 59.4	-15 45	0	NRAO local cloud
23	-11	12 31.8	+08 28	0	Arecibo
24	11	01 31.1	+30 24	21	Owens Valley, M33
25	11	00 44.5	-21 00	-4	Effelsberg, local cloud
26	-13	01 58.4	+28 35	0	NRAO
27	-13	12 03.4	+47 45	0	NRAO
28	16	13 53.7	+ 5 16	30	Arecibo
29	16	12 39.1	+41 26	35	Effelsberg, estimated value
30	-16	10 44.1	+12 05	170	NRAO
31	16	09 01.9	+78 17	-17	Effelsberg
32	17	14 58.0	+71 50	71	Effelsberg
33	17	12 17.0	+15 19	209	Westerbork, ring H I
34	18	12 48.0	+25 46	35	Arecibo,Westerbork, Jodrell Bank
35	-19	01 40.4	+13 23	160	NRAO
36	21	12 51.6	+27 25	39	Effelsberg
37	-23	03 42.0	+67 57	39	Cambridge, local cloud
38	-24	09 16.3	+64 19	310	Westerbork; α H I: 270°
39	25	01 34.0	+15 32	25	Westerbork
40	25	08 11.0	+49 13	170	NRAO
41	26	00 40.0	+41 00	33	Cambridge, M31
42	28	12 25.8	+44 22	45	Westerbork
43	28	17 49.9	+70 10	305	NRAO
44	29	12 49.3	+26 02	46	Arecibo, Westerbork
45	29	09 29.5	+21 42	26	Effelsberg, local cloud
46	30	12 15.0	+38 05	45	Effelsberg
47	-32	12 14.4	+69 45	163	Owens Valley, local cloud
48	-33	11 03.2	+00 15	335	NRAO, local cloud
49	35	00 17.6	+59 02	43	Jodrell Bank; local cloud
50	38	10 16.9	+45 49	32	Westerbork
51	-38	13 44.4	+46 22	-6	Westerbork,Effelsberg
52	39	08 14.1	+70 52	175	Cambridge
53	-39	12 33.4	+28 14	-23	Effelsberg
54	-39	13 27.8	+47 27	-10	Westerbork, local cloud
55	-39	01 44.6	+27 05	150	Arecibo
56	-41	12 23.4	+33 49	-26	NRAO, local cloud;
57	-42	12 28.1	+41 55	335	Effelsberg
58	-43	02 40.4	+37 08	165	Westerbork
59	-43	12 16.5	+47 35	-28	Westerbork, local cloud
60	-44	13 11.2	+36 51	340	Westerbork
61	-44	12 13.0	+36 35	-30	Effelsberg
62	-50	04 27.1	+71 47	25	NRAO
63	51	08 49.6	+33 36	215	NRAO
64	52	13 55.0	+42 05	85	Westerbork
65	-55	01 56.5	+18 46	130	Arecibo
66	55	01 45.0	+27 11	65	Arecibo
67	56	10 24.8	+68 40	45	NRAO, local cloud
68	57	06 10.5	+78 22	-20	NRAO,extended envelope
69	60	07 18.5	+80 16	0	NRAO
70	60	03 55.0	+67 00	305	NRAO
71	-60	02 33.3	+38 45	327	Cambridge
72	-67	17 30.0	+07 06	30	Arecibo
73	68	00 45.1	-25 34	51	Owens Valley, local cloud
74	68	12 39.7	+32 49	86	Westerbork, local cloud
75	-72	04 17.0	+75 12	180	NRAO
76	76	10 00.8	-25 55	273	Effelsberg, local cloud
77	-77	20 33.8	+59 59	62	Owens Valley, local cloud
78	-82	12 54.2	+21 57	115	Arecibo; local cloud
79	85	10 39.5	+14 00	90	NRAO
80	-86	02 24.3	+33 21	115	Arecibo
81	-87	12 48.5	+41 23	114	Westerbork, local cloud
82	-89	07 23.6	+69 18	35	NRAO
83	-89	13 13.5	+42 17	116	Westerbork, local cloud

The distribution in position angles is such that there is a large scale dipole anisotropy. Its direction is given by

$$P_0 = (81°, +8°),$$

The median of $|\alpha_P - 90°|$ where α_P is the position angle is 28° (instead of 45°), and 74% (instead of 50%) have $|\alpha_P - 90°| < 45°$; this is a "5 σ" result.

This confirms our previous results (Fliche et al., 1982a, 1983a) based on smaller samples (≈ 20 objects), on the anisotropy of the extended H I envelopes, and tells us that this dipole anisotropy is a large scale effect (larger than the Local Super Cluster?).

4. Interpretation and conclusion

The analysis presented in the previous sections was done on projected positions of the objects on the celestial sphere. It implies a tendency for parallelism of the planes of the outermost gaseous regions of spiral and irregular galaxies.

Statistical tests on optical position angles generally gave confusing results. An explanation can be suggested by the examination of an image of the Andromeda Nebula (Fig. 11). On this figure a radio map and an optical of M 31 have been superposed and the "calculated" position angle at the location of M 31 is also marked. We observe an interesting transition in position angle:

$$\alpha_{\text{optical}} \rightarrow \alpha_{\text{radio}} \rightarrow \alpha_{\text{calculated}} .$$

The effect of warping, which is visible on the optical image is more clearly seen on the radio image which has a ∫ shape. The position angle changes from the inner part of the galaxy toward the external regions and becomes closer to the "calculated" position angle.

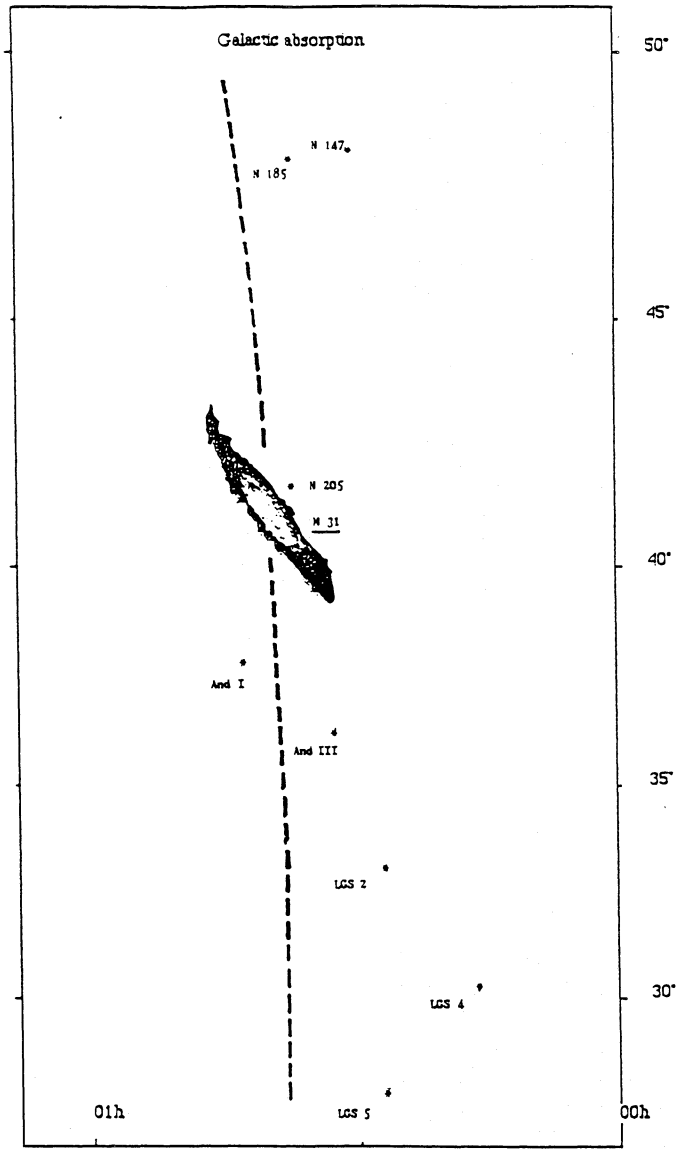

Fig. 11. Andromeda (optical + radio) and its satellites. The dotted line traces the expected meridian related to the pole P_0

Because M 31 is very close to us we can observe dwarf galaxies which constitute the M 31 satellite system. The apparent spatial extension of this system is larger than 30° and very elongated. It is also much larger than the radio image. The point we want to make about this system is shown in Fig. 11: the distribution of the satellites galaxies seem to prolong the warp of M 31. Moreover it seems that such elongated systems are not unique (for the Galaxy, see Fliche et al., 1982a; M 83: Fliche et al., 1983a).

Our observational results suggest that the parallelism can be better found in the outermost parts of galaxies. This might be understood in a scenario where galaxies are formed by condensation in a stratified medium. The stratification would be perpendicular to the pole P_0. If this interpretation is correct, this stratification should be searched for larger scales.

A large fraction of our sample is located in the Local Super Cluster which is flat and has a pole at S: (103°, −16°). This direction is more than 30° off our pole and leaves open the question of the definition of the supergalactic pole.

In previous works (Souriau, 1979; Fliche et al., 1982b), we determined a "cosmic" pole:

Ω: (86°, +7°)

deduced from extremely distant objects (quasars with redshift between 1 and 3). New data (Véron et al., 1987) did not change this result. As a matter of fact this pole Ω is very near the pole obtained in this paper. It is therefore possible that the dipole anisotropy detected here is of cosmological origin; some other facts seems to be compatible with this hypothesis (kinematics and spatial distribution of galaxies). However a more general discussion on this subject would be beyond the scope of the present paper.

Acknowledgements. We thank Edmond Giraud and James Lequeux who helped us in the preparation of this text.

References

Fliche, H.H., Souriau, J.M., Triay, R.: 1982a, *Astron. Astrophys.* **108**, 256

Fliche, H.H., Souriau, J.M., Triay, R.: 1982b, C.N.R.S.-C.P.T. 82 preprint, p. 1402

Fliche, H.H., Souriau, J.M., Triay, R.: 1983a, *Journées Relativistes*, eds. S. Benenti, M. Ferreris, M. Francaviglia, Turin

Fliche, H.H., Souriau, J.M.: 1983b, *Clusters and groups of galaxies*, eds. Mardirossian et al., Reidel, Dordrecht, p. 77

Mac Gillivray, H.T., Dodd, R.J., Mac Nally, B.V., Corwin, Jr, H.G.: 1982, *Monthly Notices Roy. Astron. Soc.* **198**, 605

Souriau, J.M.: 1979, *Coll. Internat. C.N.R.S.* "EINSTEIN", p. 197

Véron-Cetty, M.P., Véron, P.: 1987, *Catalog of quasars and active nuclei*, 3nd ed., *E.S.O. Scientific reports* **5**